The Design of Sum-of-Cisoids Rayleigh Fading Channel Simulators Assuming Non-Isotropic Scattering Conditions

Carlos A. Gutiérrez, *Member, IEEE*, and Matthias Pätzold, *Senior Member, IEEE*

***Abstract*—In this letter, we introduce the Riemann sum method (RSM) as an effective tool for the design of sum-of-cisoids (SOC) simulators for narrowband mobile Rayleigh fading channels under non-isotropic scattering conditions. We compare the performance of the RSM with that of the generalized method of equal areas (GMEA) and the L_p-norm method (LPNM), which were until now the only methods available for the design of SOC simulators for non-isotropic scattering channels. The obtained results indicate that the RSM is better suited than the GMEA and the LPNM to emulate the channel's autocorrelation function (ACF), whereas the latter two methods are more precise regarding the approximation of the envelope distribution. The results also show that the benefits of increasing the number of cisoids are more significant in the case of the RSM than in the case of the GMEA and LPNM. Owing to its simplicity and good performance, the RSM can be used to design flexible simulation platforms for the laboratory analysis of mobile communication systems operating in non-isotropic scattering environments.**

***Index Terms*—Channel simulators, mobile communications, non-isotropic scattering, fading channels, sum-of-cisoids, sum-of-sinusoids.**

I. Introduction

SIMULATION MODELS having the ability to reproduce the statistical properties of non-isotropic scattering channels are highly desirable for the software-assisted performance analysis of modern mobile communication systems. They are important, for example, to assess the performance of handover algorithms and speed estimation techniques under realistic propagation scenarios in which the quadrature components of the channel's complex envelope are cross-correlated [1].

It has been shown in a number of papers, e.g., [2]–[5], that the simulation of non-isotropic scattering channels can efficiently be performed by means of a finite sum of complex sinusoids (cisoids). Sum-of-cisoids (SOC) models are closely related to the electromagnetic plane-wave propagation model [6]. They provide an excellent basis not only for enabling the simulation of narrowband single-input single-output (SISO) channels [3], but also for the simulation of wideband multiple-input multiple-output (MIMO) channels [5]. The interested reader can find detailed background information on the theory behind the design of SOC simulators for mobile fading channels in [7].

Currently, there exist only two parameter computation methods suitable for the design of SOC simulators for non-isotropic scattering channels, namely the L_p-norm method (LPNM) [2] and the generalized method of equal areas (GMEA) [3], [7]. Both methods produce good results regarding the emulation of the channel's statistics [2]–[5]. Nonetheless, the LPNM relies upon numerical optimization techniques that make the determination of the model parameters a time-consuming task. In contrast to this, the GMEA requires a comparatively large number of cisoids to properly emulate the channel's correlation properties. The development of new methods, under the constraint of simplicity and accuracy, is therefore desirable to facilitate the performance analysis of modern and forthcoming mobile communication systems operating in non-isotropic scattering environments.

In this letter, we introduce a simple and effective method for the design of SOC simulators for mobile Rayleigh fading channels under the assumption of non-isotropic scattering conditions. The proposed method, which is based on a Riemann sum approximation of the channel's autocorrelation function (ACF), is presented here in the context of SISO channels. Its extension to the design of MIMO channel simulators is straightforward. We evaluate the performance of the Riemann sum method (RSM) with respect to its accuracy and efficiency for emulating the ACF and the envelope distribution of the channel. In addition, we compare its performance with that of the GMEA and the LPNM. With no loss of generality, we carry out our investigations by assuming that the channel's angle of arrival (AOA) statistics follows the von Mises distribution [8]. The obtained results show that the GMEA and the LPNM are more precise than the RSM regarding the approximation of the envelope distribution. However, the RSM outperforms the other two methods when it comes to the emulation of the channel's ACF. Our investigations also indicate that the benefits of increasing the number of cisoids are more significant in the case of the RSM than in the case of the GMEA and LPNM.

The rest of the paper is organized as follows. Sections II and III review the characteristics of the reference channel model and the SOC simulation model, respectively. Section IV introduces the RSM. Its performance is evaluated in Section V. Finally, the main points are summarized in Section VI.

II. The Reference Model

Our reference model is a small-scale frequency-nonselective Rayleigh fading channel. We model the channel's complex

Manuscript received August 10, 2009; revised November 10, 2009; accepted January 25, 2010. The associate editor coordinating the review of this letter and approving it for publication was K. K. Wong.

Parts of this paper were presented at the 2009 International Workshop on Mobile Computing and Networking Technologies (WMCNT'09), St. Petersburg, Russia.

C. A. Gutiérrez is with the School of Engineering, Universidad Panamericana, Campus Bonaterra, Josemaría Escrivá de Balaguer No. 101, Aguascalientes 20290, Mexico (e-mail: cagutierrez@up.edu.mx).

M. Pätzold is with the Department of Information and Communication Technology, Faculty of Engineering and Science, University of Agder, P.O. Box 509, 4898 Grimstad, Norway (e-mail: matthias.paetzold@uia.no).

Digital Object Identifier 10.1109/TWC.2010.04.091198

envelope in the equivalent baseband by a stationary zero-mean complex Gaussian process[1] $\boldsymbol{\mu}(t)$ with variance $\sigma_{\boldsymbol{\mu}}^2$. Following Clarke's two-dimensional scattering propagation model [9], and invoking the central limit theorem [10, pp. 281–290], we can express the complex Gaussian process $\boldsymbol{\mu}(t)$ as a series of horizontally traveling plane waves as follows

$$\boldsymbol{\mu}(t) \;=\; \lim_{N\to\infty} \frac{\sigma_{\boldsymbol{\mu}}}{\sqrt{N}} \sum_{n=1}^{N} \exp\left\{j(2\pi \boldsymbol{f}_n t + \boldsymbol{\theta}_n)\right\}. \quad (1)$$

In line with Clarke's model, we define the phases $\boldsymbol{\theta}_n$ in (1) as independent random variables uniformly distributed on $[-\pi, \pi)$. The Doppler frequencies $\boldsymbol{f}_n$ are defined as $\boldsymbol{f}_n \triangleq f_{\max}\cos(\boldsymbol{\alpha}_n)$, $n = 1, 2, \ldots, N$, where $f_{\max}$ is the maximum Doppler shift due to the movement of the receiver, and $\boldsymbol{\alpha}_n$ is the AOA of the nth incident wave. The AOAs $\boldsymbol{\alpha}_n$ are assumed to be independent and identically distributed (i.i.d.) random variables. In addition, the AOAs $\boldsymbol{\alpha}_n$ and the phases $\boldsymbol{\theta}_n$ are considered as being statistically independent.

The reference model can be characterized by means of the ACF $r_{\boldsymbol{\mu}\boldsymbol{\mu}}(\tau) \triangleq E\{\boldsymbol{\mu}^*(t)\,\boldsymbol{\mu}(t+\tau)\}$ of $\boldsymbol{\mu}(t)$; $E\{\cdot\}$ denotes statistical expectation and $(\cdot)^*$ the complex conjugate. One can verify that [7, Sec. 2.3.1]

$$r_{\boldsymbol{\mu}\boldsymbol{\mu}}(\tau) \;=\; 2\,\sigma_{\boldsymbol{\mu}}^2 \int_0^{\pi} g_{\boldsymbol{\alpha}}(\alpha)\, \exp\left\{j2\pi f_{\max}\cos(\alpha)\tau\right\} d\alpha \quad (2)$$

where $g_{\boldsymbol{\alpha}}(\alpha)$ is the even part of the probability density function (PDF) of the AOA $p_{\boldsymbol{\alpha}}(\alpha)$, i.e., $g_{\boldsymbol{\alpha}}(\alpha) \triangleq [p_{\boldsymbol{\alpha}}(\alpha) + p_{\boldsymbol{\alpha}}(-\alpha)]/2$. The von Mises distribution has been shown to be an adequate model for the AOA statistics of mobile fading channels in both isotropic and non-isotropic scattering environments [8]. In this paper, we will consider such a distribution to demonstrate the performance of the RSM. The von Mises PDF and its even part are given, in that order, by:

$$p_{\boldsymbol{\alpha}}^{\mathrm{VM}}(\alpha) \;\triangleq\; \frac{\exp\left\{\kappa\cos(\alpha - m_\alpha)\right\}}{2\pi I_0(\kappa)} \quad (3)$$

$$g_{\boldsymbol{\alpha}}^{\mathrm{VM}}(\alpha) \;=\; \frac{\exp\left\{\kappa\cos(\alpha)\cos(m_\alpha)\right\}}{2\pi I_0(\kappa)} \times \cosh\left(\kappa\sin(\alpha)\sin(m_\alpha)\right) \quad (4)$$

for $\alpha \in [-\pi, \pi)$. The parameter $m_\alpha \in [-\pi, \pi)$ designates the mean AOA, $\kappa \geq 0$ determines the angular spread, and $I_0(\cdot)$ is the zeroth order modified Bessel function of the first kind. By substituting (4) into (2), we obtain the following closed-form expression for the ACF of $\boldsymbol{\mu}(t)$ [8]:

$$r_{\boldsymbol{\mu}\boldsymbol{\mu}}(\tau) \;=\; \frac{\sigma_{\boldsymbol{\mu}}^2}{I_0(\kappa)}\, I_0\Big(\left\{\kappa^2 - (2\pi f_{\max}\tau)^2 + j4\pi\kappa f_{\max}\cos(m_\alpha)\tau\right\}^{1/2}\Big). \quad (5)$$

Under isotropic scattering conditions ($\kappa = 0$), the ACF defined in (5) reduces to $r_{\boldsymbol{\mu}\boldsymbol{\mu}}(\tau) = \sigma_{\boldsymbol{\mu}}^2\, J_0(2\pi f_{\max}\tau)$, where $J_0(\cdot)$ denotes the zeroth order Bessel function of the first kind.

Regarding the distributions of the envelope $\boldsymbol{\zeta}(t) \triangleq |\boldsymbol{\mu}(t)|$ and phase $\boldsymbol{\phi}(t) \triangleq \arg\{\boldsymbol{\mu}(t)\}$ of $\boldsymbol{\mu}(t)$, one can demonstrate that irrespective of the AOA statistics, the PDFs of $\boldsymbol{\zeta}(t)$ and $\boldsymbol{\phi}(t)$ are given by [11, Sec. 6.1.1]:

$$p_{\boldsymbol{\zeta}}(z) \;=\; \frac{2\,z}{\sigma_{\boldsymbol{\mu}}^2}\cdot\exp\left\{-\frac{z^2}{\sigma_{\boldsymbol{\mu}}^2}\right\}, \qquad z \geq 0 \quad (6)$$

$$p_{\boldsymbol{\phi}}(\theta) \;=\; \frac{1}{2\pi}, \qquad \phi \in [-\pi, \pi) \quad (7)$$

respectively. Equation (6) can be identified as the Rayleigh PDF [10, p. 113], whereas the PDF in (7) is the uniform density for circular variates [12, Sec. 3.5.3].

III. The SOC-Based Simulation Model

One may observe from (1) that a hardware/software realization of the reference model described by $\boldsymbol{\mu}(t)$ is not possible, as it requires the implementation of a sum of an infinite number of cisoids. Fortunately, most of the statistical properties of $\boldsymbol{\mu}(t)$ relevant for system performance analysis—such as the correlation properties and the distributions of the envelope and phase—can be approximated by a simulation model comprising a finite SOC. In this paper, we will consider a stochastic SOC simulation model of the form

$$\hat{\boldsymbol{\mu}}(t) \;=\; \sum_{n=1}^{N} \hat{c}_n \exp\left\{j(2\pi\hat{f}_n t + \hat{\boldsymbol{\theta}}_n)\right\}. \quad (8)$$

The phases $\hat{\boldsymbol{\theta}}_n$ introduced above are defined as i.i.d. random variables, each having a uniform distribution over $[-\pi, \pi)$, whereas the Doppler frequencies $\hat{f}_n$ are given as $\hat{f}_n \triangleq f_{\max}\cos(\hat{\alpha}_n)$, $n = 1, 2, \ldots, N$, where $\hat{\alpha}_n \in [0, \pi)$. To ensure that the variance of $\hat{\boldsymbol{\mu}}(t)$ equals that of the reference model, it is assumed that the cisoids' gains $\hat{c}_n$ satisfy the boundary condition $\sum_{n=1}^{N} \hat{c}_n^2 = \sigma_{\boldsymbol{\mu}}^2$ [13, Sec. III.A].

The statistical properties of the SOC model in (8) have thoroughly been investigated in [13]. In that paper, it is shown that $\hat{\boldsymbol{\mu}}(t)$ is a wide-sense stationary (WSS) process with mean zero and variance $\sigma_{\boldsymbol{\mu}}^2$. In addition, it is demonstrated that the ACF $r_{\hat{\boldsymbol{\mu}}\hat{\boldsymbol{\mu}}}(\tau) \triangleq E\{\hat{\boldsymbol{\mu}}^*(t)\hat{\boldsymbol{\mu}}(t+\tau)\}$, the PDF $p_{\hat{\boldsymbol{\zeta}}}(z)$ of the envelope $\hat{\boldsymbol{\zeta}}(t) \triangleq |\hat{\boldsymbol{\mu}}(t)|$, and the PDF $p_{\hat{\boldsymbol{\phi}}}(\hat{\theta})$ of the phase $\hat{\boldsymbol{\phi}}(t) \triangleq \arg\{\hat{\boldsymbol{\mu}}(t)\}$ of $\hat{\boldsymbol{\mu}}(t)$ are equal to:

$$r_{\hat{\boldsymbol{\mu}}\hat{\boldsymbol{\mu}}}(\tau) \;=\; \sum_{n=1}^{N} \hat{c}_n^2 \exp\left\{j2\pi f_{\max}\cos(\hat{\alpha}_n)\tau\right\} \quad (9)$$

$$p_{\hat{\boldsymbol{\zeta}}}(z) \;=\; z(2\pi)^2 \int_0^{\infty} \left[\prod_{n=1}^{N} J_0(2\pi|\hat{c}_n|x)\right] \times J_0(2\pi z x)\, x\, dx, \qquad z \geq 0 \quad (10)$$

$$p_{\hat{\boldsymbol{\phi}}}(\hat{\theta}) \;=\; \frac{1}{2\pi}, \qquad \hat{\theta} \in [-\pi, \pi) \quad (11)$$

respectively. Simulation results presented in [13] indicate that the envelope PDF defined in (10) is in good agreement with the Rayleigh PDF $p_{\boldsymbol{\zeta}}(z)$ for values of N as small as ten if $\hat{c}_n = \sigma_{\boldsymbol{\mu}}/\sqrt{N}$. In fact, it is demonstrated in [13] that if $\hat{c}_n = \sigma_{\boldsymbol{\mu}}/\sqrt{N}$, then $p_{\hat{\boldsymbol{\zeta}}}(z) \to p_{\boldsymbol{\zeta}}(z)$ as $N \to \infty$.

Without going into details, we observe that the stochastic SOC simulator described by $\hat{\boldsymbol{\mu}}(t)$ is mean-ergodic and autocorrelation-ergodic on the condition that the Doppler frequencies $\hat{f}_n$ satisfy the inequalities $\hat{f}_n \neq 0\ \forall n$ and $\hat{f}_n \neq \hat{f}_m$,

[1]Throughout the paper, we will make use of bold symbols and letters to denote random variables and stochastic processes, whereas we will employ normal symbols and letters for constants and deterministic processes.

$n \neq m$. For further information, we refer the reader to [7, Sec. 3.5].

IV. The Riemann Sum Method

A. Basic Approach

The problem at hand consists in finding values for the Doppler frequencies $\hat{f}_n$ (or equivalently, for the AOAs $\hat{\alpha}_n$) and the gains $\hat{c}_n$ of the SOC simulation model defined in (8) that allow for a proper emulation of the statistical properties of the reference model. To solve this problem, we will assume that the PDF of the AOA $p_{\boldsymbol{\alpha}}(\alpha)$ contains no singularities, so that one can regard the integral in (2) as being a proper integral. Under this consideration, $r_{\boldsymbol{\mu}\boldsymbol{\mu}}(\tau)$ can be written as a midpoint Riemann sum of the form

$$\begin{aligned} r_{\boldsymbol{\mu}\boldsymbol{\mu}}(\tau) &= \lim_{N\to\infty} \frac{2\pi\sigma_{\boldsymbol{\mu}}^2}{N} \sum_{n=1}^{N} g_{\boldsymbol{\alpha}}\left(\frac{\pi}{N}\left[n-\frac{1}{2}\right]\right) \\ &\quad \times \exp\left\{j2\pi f_{\max}\cos\left(\frac{\pi}{N}\left[n-\frac{1}{2}\right]\right)\tau\right\}. \end{aligned}$$

If we remove the limit $N \to \infty$ from the equation above, then we may presume that

$$\begin{aligned} r_{\boldsymbol{\mu}\boldsymbol{\mu}}(\tau) &\approx \frac{2\pi\sigma_{\boldsymbol{\mu}}^2}{N} \sum_{n=1}^{N} g_{\boldsymbol{\alpha}}\left(\frac{\pi}{N}\left[n-\frac{1}{2}\right]\right) \\ &\quad \times \exp\left\{j2\pi f_{\max}\cos\left(\frac{\pi}{N}\left[n-\frac{1}{2}\right]\right)\tau\right\}. \quad (12) \end{aligned}$$

A comparison of (9) and (12) suggests that the ACF $r_{\hat{\boldsymbol{\mu}}\hat{\boldsymbol{\mu}}}(\tau)$ of the simulation model will render a good approximation to $r_{\boldsymbol{\mu}\boldsymbol{\mu}}(\tau)$ if we choose:

$$\hat{\alpha}_n = \frac{\pi}{N}\left(n-\frac{1}{2}\right) \quad (13)$$

$$\hat{c}_n = \frac{\sigma_{\boldsymbol{\mu}}}{c_\Sigma}\sqrt{\frac{2\pi}{N} g_{\boldsymbol{\alpha}}(\hat{\alpha}_n)} \quad (14)$$

for $n = 1, 2, \ldots, N$, where c_Σ is a normalization parameter introduced to guarantee the fulfillment of the equality $\sum_{n=1}^{N} \hat{c}_n^2 = \sigma_{\boldsymbol{\mu}}^2$. By substituting $\hat{c}_n$ from (14) into the aforementioned equality, we find that $c_\Sigma = \sqrt{\frac{2\pi}{N}\sum_{m=1}^{N} g_{\boldsymbol{\alpha}}(\hat{\alpha}_m)}$. Taking this into account, we can rewrite (14) simply as

$$\hat{c}_n = \sigma_{\boldsymbol{\mu}}\sqrt{\frac{g_{\boldsymbol{\alpha}}(\hat{\alpha}_n)}{\sum_{m=1}^{N} g_{\boldsymbol{\alpha}}(\hat{\alpha}_m)}}, \quad n = 1, 2, \ldots, N. \quad (15)$$

The methodology given by (13) and (15) establishes a parameter computation method that we will refer to as the basic RSM (BRSM). It is worth mentioning that the idea behind the BRSM has recently been applied in [14] to simulate mobile MIMO Rayleigh fading channels, yielding remarkable results concerning the emulation of the spatial cross-correlation function and the temporal ACF.

It is evident that if the parameters of $\hat{\boldsymbol{\mu}}(t)$ are computed by applying the BRSM, then $r_{\hat{\boldsymbol{\mu}}\hat{\boldsymbol{\mu}}}(\tau) \to r_{\boldsymbol{\mu}\boldsymbol{\mu}}(\tau)$ as $N \to \infty$. Furthermore, by invoking Lyapunov's central limit theorem [15, p. 146], one can state that in the limit when $N \to \infty$, the quadrature components of $\hat{\boldsymbol{\mu}}(t)$ are Gaussian processes with zero mean and variance $\sigma_{\boldsymbol{\mu}}^2/2$. Hence, we can presume that $p_{\hat{\boldsymbol{\zeta}}}(z) \to p_{\boldsymbol{\zeta}}(z)$ as $N \to \infty$. For a finite number of cisoids, we have experimentally observed that irrespective of the AOA statistics, the BRSM produces an excellent approximation to the ACF of $\boldsymbol{\mu}(t)$ for $\tau \in \left[-\frac{N}{4f_{\max}}, \frac{N}{4f_{\max}}\right]$. However, we have also observed that the BRSM performs poorly regarding the emulation of the envelope distribution of $\boldsymbol{\mu}(t)$ if the angular spread is small, i.e., if the scattering is highly non-isotropic. Under such circumstances, there is a significant difference among the gains $\hat{c}_n$ of $\hat{\boldsymbol{\mu}}(t)$. This characteristic does not entail any problems for the emulation of $r_{\boldsymbol{\mu}\boldsymbol{\mu}}(\tau)$, but it does affect the effectiveness of the simulation model for approximating the PDF of $\boldsymbol{\zeta}(t)$, as the best fitting of $p_{\hat{\boldsymbol{\zeta}}}(z)$ against the Rayleigh density $p_{\boldsymbol{\zeta}}(z)$ is obtained if all gains $\hat{c}_n$ have the same value, i.e., if $\hat{c}_n = \sigma_{\boldsymbol{\mu}}/\sqrt{N}$ [13]. Figure 1 exemplifies the problem by considering the von Mises PDF.

B. Improved Approach

To improve the quality of the approximation $p_{\hat{\boldsymbol{\zeta}}}(z) \approx p_{\boldsymbol{\zeta}}(z)$, we have to impose a constraint on the range of values that the gains $\hat{c}_n$ can take. With this in mind, we will assume that the PDF of the AOA is defined in such a way that its even part $g_{\boldsymbol{\alpha}}(\alpha)$ has at most one maximum in $[0, \pi)$. Thereby, for a given threshold $\gamma \in \left(0, \sup\{g_{\boldsymbol{\alpha}}(\alpha)\}_{\alpha\in[0,\pi)}\right)$, where $\sup\{\cdot\}$ denotes the supremum, we can identify one and only one subinterval $\mathcal{I}_U$ in $[0, \pi)$ satisfying $g_{\boldsymbol{\alpha}}(\alpha) > \gamma$, $\forall \alpha \in \mathcal{I}_U$, meaning that $g_{\boldsymbol{\alpha}}(\alpha)$ is above the threshold only within $\mathcal{I}_U$.[2] If the threshold is chosen low, so that $g_{\boldsymbol{\alpha}}(\alpha) \approx 0$ $\forall \alpha \notin \mathcal{I}_U$, then one can state that

$$r_{\boldsymbol{\mu}\boldsymbol{\mu}}(\tau) \approx \sigma_{\boldsymbol{\mu}}^2 \int_{\alpha\in\mathcal{I}_U} g_{\boldsymbol{\alpha}}(\alpha)\, \exp\{j2\pi f_{\max}\cos(\alpha)\tau\}\, d\alpha. \quad (16)$$

In this case, it makes sense to compute the AOAs $\hat{\alpha}_n$ of $\hat{\boldsymbol{\mu}}(t)$ by taking into account only the subinterval $\mathcal{I}_U$. Thereby, we may reduce the range of the gains $\hat{c}_n$ in (15) while keeping a good approximation to $r_{\boldsymbol{\mu}\boldsymbol{\mu}}(\tau)$. Following this reasoning, we redefine the AOAs $\hat{\alpha}_n$ as follows

$$\hat{\alpha}_n = \alpha_\ell + \frac{\alpha_u - \alpha_\ell}{N}\left(n-\frac{1}{2}\right), \quad \alpha_u > \alpha_\ell \quad (17)$$

for $n = 1, 2, \ldots, N$, where α_ℓ and α_u designate the lower and the upper boundaries of $\mathcal{I}_U$. The quantities α_ℓ and α_u are to be found by identifying the points in $[0, \pi)$ at which the function $g_{\boldsymbol{\alpha}}(\alpha)$ crosses the threshold γ from down to up (corresponding to α_ℓ) and/or from up to down (corresponding to α_u). If no up-crossing is observed, then $\alpha_\ell = 0$, whereas $\alpha_u = \pi$ if no down-crossing occurs.

The methodology resulting in (15) and (17) constitutes the RSM. For this method, we can state on the basis of Lyapunov's central limit theorem that $p_{\hat{\boldsymbol{\zeta}}}(z) \to p_{\boldsymbol{\zeta}}(z)$ as $N \to \infty$, as in the case of the BRSM. However, for the RSM, we have that if $\int_{\alpha\notin\mathcal{I}_U} g_{\boldsymbol{\alpha}}(\alpha)d\alpha \neq 0$, then $\lim_{N\to\infty} r_{\hat{\boldsymbol{\mu}}\hat{\boldsymbol{\mu}}}(\tau) \neq r_{\boldsymbol{\mu}\boldsymbol{\mu}}(\tau)$.

It is worth mentioning that under isotropic scattering conditions, the RSM reduces to the extended method of exact

[2]This consideration is in line with the characteristics of several important theoretical models for the distribution of the AOA, such as those described in [12, Sec. 3.5] and [16]. However, for some empirical models derived from measured data, various disjoint subintervals $\mathcal{I}_{U,m}$, $m = 1, 2, \ldots, M$, could be identified in $[0, \pi)$ satisfying $g_{\boldsymbol{\alpha}}(\alpha) \geq \gamma$ $\forall \alpha \in \mathcal{I}_{U,m}$. We recognize the importance of designing measurement-based channel simulation models, but we leave this problem for future research, as it is beyond the scope of this letter.

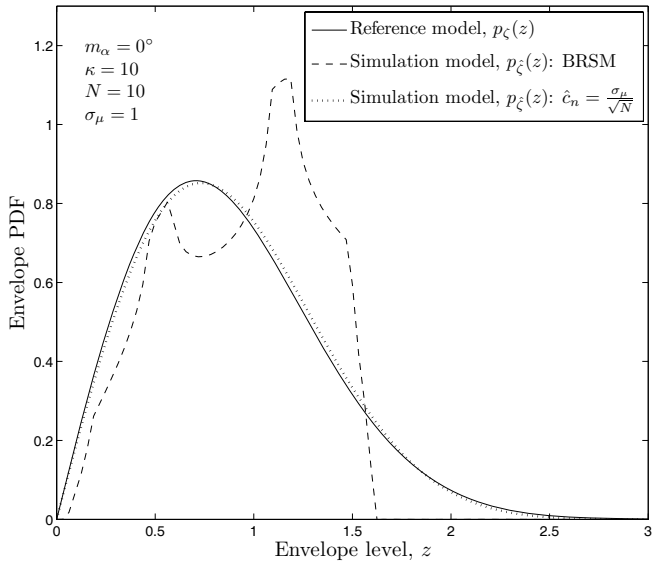

Fig. 1. Comparison between the Rayleigh PDF $p_{\boldsymbol{\zeta}}(z)$ and the envelope PDF $p_{\hat{\boldsymbol{\zeta}}}(z)$ of the simulation model by applying the BRSM to the von Mises PDF of the AOA with parameters $m_\alpha = 0°$ and $\kappa = 10$ (severe non-isotropic scattering conditions).

Doppler spread (EMEDS) [4], which is a parameter computation method that exactly reproduces the Doppler spread of isotropic scattering channels for any value of N. These two methods are actually based on the same approach, since the EMEDS has been derived from a Riemann sum approximation of the ACF $r_{\boldsymbol{\mu}\boldsymbol{\mu}}(\tau) = \sigma_{\boldsymbol{\mu}}^2 J_0(2\pi f_{\max}\tau)$ characterizing isotropic scattering channels. However, the EMEDS cannot be used directly to design simulation models for non-isotropic scattering channels.

C. Computation of the Threshold

Choosing a proper value for the threshold γ is clearly the critical step in the RSM. In fact, when setting the threshold, one has to be aware of the fact that the method will be affected by the same problems of the BRSM if γ is too small. On the other hand, if γ is large, then the RSM will become more precise regarding the approximation of the envelope distribution of $\boldsymbol{\mu}(t)$, but it will loose accuracy with respect to the emulation of $r_{\boldsymbol{\mu}\boldsymbol{\mu}}(\tau)$. Keeping this in mind, we propose to compute γ as a percentage q of the largest value (supremum) of $g_{\boldsymbol{\alpha}}(\alpha)$, i.e.,

$$\gamma \quad = \quad \sup\{g_{\boldsymbol{\alpha}}(\alpha)\} \times \frac{q}{100}, \qquad 0 < q < 100. \tag{18}$$

A good trade-off between the approximations $p_{\hat{\boldsymbol{\zeta}}}(z) \approx p_{\boldsymbol{\zeta}}(z)$ and $r_{\hat{\boldsymbol{\mu}}\hat{\boldsymbol{\mu}}}(\tau) \approx r_{\boldsymbol{\mu}\boldsymbol{\mu}}(\tau)$ can be obtained by choosing $q \in [0.1, 1]$. By doing so, we will introduce only a small degradation to the relationship in (16), and the maximum value of the gains $\hat{c}_n$ relative to the minimum will be constrained between 20 dB (when $q = 1$) and 30 dB (when $q = 0.1$). In comparison with the BRSM, this is a significant reduction in the range of values of the gains $\hat{c}_n$, since for such a method the quotient $\max\{\hat{c}_n\}/\min\{\hat{c}_n\}$ can be as large as 200 dB when the scattering is highly non-isotropic [7, p. 55]. We will employ the notation γ_q to indicate that the threshold equals q percent of the supremum of $g_{\boldsymbol{\alpha}}(\alpha)$.

V. Performance Evaluation

A. Considerations

In this section, we present a performance comparison among the RSM, the GMEA [3], and the LPNM [2] in terms of the emulation of the reference model's ACF $r_{\boldsymbol{\mu}\boldsymbol{\mu}}(\tau)$ and envelope distribution[3] $p_{\boldsymbol{\zeta}}(z)$. We consider the simulation of three different propagation scenarios that exhibit severe non-isotropic scattering conditions. The AOA statistics of such scenarios are characterized by the von Mises PDF with $\kappa = 10$ and $m_\alpha \in \{0°, 30°, 90°\}$. The parameters $m_\alpha = 90°$ and $\kappa = 10$ are associated to a fading channel having a complex envelope with uncorrelated quadrature components. The other two parameter constellations correspond to channels whose complex envelopes have cross-correlated quadrature components [7].

For the GMEA, the cisoids' gains $\hat{c}_n$ are given by [3], [7]

$$\hat{c}_n \quad = \quad \frac{\sigma_{\boldsymbol{\mu}}}{\sqrt{N}}, \quad n = 1, 2, \ldots, N \tag{19}$$

whereas the AOAs $\hat{\alpha}_n$ are to be found by numerically solving the equation

$$\int_0^{\hat{\alpha}_n} g_{\boldsymbol{\alpha}}^{\mathrm{VM}}(\alpha)\, d\alpha - \frac{1}{2N}\left(n - \frac{1}{2}\right) = 0, \quad n = 1, 2, \ldots, N. \tag{20}$$

The LPNM, as presented in [2], also specifies the gains $\hat{c}_n$ as in (19), but the parameters $\hat{\alpha}_n$ (or $\hat{f}_n$) should be computed such that the following L_p-norm error function is minimized

$$\epsilon_{r_{\boldsymbol{\mu}\boldsymbol{\mu}}}^{(p)} \quad \triangleq \quad \left\{ \frac{1}{\tau_{\max}} \int_0^{\tau_{\max}} |r_{\boldsymbol{\mu}\boldsymbol{\mu}}(\tau) - r_{\hat{\boldsymbol{\mu}}\hat{\boldsymbol{\mu}}}(\tau)|^p \, d\tau \right\}^{1/p} \tag{21}$$

where p is a positive integer and $\tau_{\max} > 0$ determines the length of the interval $[0, \tau_{\max}]$ inside of which the approximation $r_{\boldsymbol{\mu}\boldsymbol{\mu}}(\tau) \approx r_{\hat{\boldsymbol{\mu}}\hat{\boldsymbol{\mu}}}(\tau)$ is of interest. The minimization of $\epsilon_{r_{\boldsymbol{\mu}\boldsymbol{\mu}}}^{(p)}$ has to be done by applying a numerical optimization algorithm, e.g., that described in [17], which can efficiently be implemented in MATLAB® by using the `fminsearch` function. In our simulations, we employed the Doppler frequencies defined by the GMEA as initial values to minimize (21). In addition, we set $p = 2$ and $\tau_{\max} = N/(4f_{\max})$. There exist several different variants of the LPNM, which are revised in [11]. In this paper, we will focus our attention on the original version described in [2], as it is the one that is more commonly used. However, a performance comparison between the RSM and the most efficient variants of the LPNM can be found in [7]. The conclusions presented in [7] are the same as the ones drawn here.

For the RSM, we will consider a threshold $\gamma_{0.5}$ if not otherwise stated.

[3]We do not pay attention to the emulation of the phase PDF $p_{\boldsymbol{\phi}}(\theta)$, as it follows from (7) and (11) that the equality $p_{\hat{\boldsymbol{\phi}}}(\theta) = p_{\boldsymbol{\phi}}(\theta)$ holds regardless of the simulation model's parameters.

B. Emulation of the ACF

The absolute value of the ACF of the reference model, $|r_{\boldsymbol{\mu}\boldsymbol{\mu}}(\tau)|$ [see (5)], is plotted in Fig. 2 against the absolute value of the ACF of the simulation model, $|r_{\hat{\boldsymbol{\mu}}\hat{\boldsymbol{\mu}}}(\tau)|$ [see (9)], by applying each of the three methods under consideration with $N = 10$. One can observe from the graphs depicted in Fig. 2 that the RSM outperforms the LPNM and the GMEA concerning the emulation of $r_{\boldsymbol{\mu}\boldsymbol{\mu}}(\tau)$. In fact, in the case of the RSM, no differences between $|r_{\boldsymbol{\mu}\boldsymbol{\mu}}(\tau)|$ and $|r_{\hat{\boldsymbol{\mu}}\hat{\boldsymbol{\mu}}}(\tau)|$ are visible for $\tau < 2.5/f_{\max}$.

The root mean square error (RMSE) $\epsilon^{(2)}_{r_{\boldsymbol{\mu}\boldsymbol{\mu}}}$ of the simulation model's ACF [see (21)] is plotted in Fig. 3 as a function of N. For the RSM, we have evaluated the RMSE $\epsilon^{(2)}_{r_{\boldsymbol{\mu}\boldsymbol{\mu}}}$ by considering γ_1, $\gamma_{0.5}$, and $\gamma_{0.1}$. The graphs presented in Fig. 3 show that the RMSE corresponding to the RSM is considerably smaller than that associated with the GMEA and the LPNM. Moreover, it can be noticed from the curves shown in that figure that the performance improvement obtained by increasing the number of cisoids is more significant in the case of the RSM than in the case of the other two methods.

C. Emulation of the Envelope Distribution

Figure 4 shows a comparison between the envelope PDF of the reference model, $p_{\boldsymbol{\zeta}}(z)$ [see (6)], and the envelope PDF of the simulation model, $p_{\hat{\boldsymbol{\zeta}}}(z)$ [see (10)], with $N = 10$ and $\sigma^2_{\boldsymbol{\mu}} = 1$. We observe that the GMEA and the LPNM result in exactly the same PDF of $\hat{\boldsymbol{\zeta}}(t)$ for all scenarios. This is due to the fact that the envelope PDF of the simulation model is solely influenced by the set of gains $\{\hat{c}_n\}$ [see (10)], and both the GMEA and the LPNM define the cisoids' gains in the same way irrespective of the channel's AOA statistics. The results presented in Fig. 4 show that the LPNM and the GMEA produce a better approximation to the PDF of $\boldsymbol{\zeta}(t)$ than the RSM, although the performance of the RSM is quite good.

In order to quantitatively measure the methods' performance, we have plotted in Fig. 5 the RMSE

$$\epsilon^{(2)}_{p_{\boldsymbol{\zeta}}} \triangleq \left\{ \int_0^{\infty} \left| p_{\boldsymbol{\zeta}}(z) - p_{\hat{\boldsymbol{\zeta}}}(z) \right|^2 dz \right\}^{1/2} \tag{22}$$

between $p_{\boldsymbol{\zeta}}(z)$ and $p_{\hat{\boldsymbol{\zeta}}}(z)$. Again, for the RSM, we have considered γ_1, $\gamma_{0.5}$, and $\gamma_{0.1}$. One may observe from Fig. 5 that the RSM causes the largest error. Even though the RMSE $\epsilon^{(2)}_{p_{\boldsymbol{\zeta}}}$ registered by this method is rather small, it is about two times higher than the one produced by the other two methods.

D. Time Required for Computing the Model Parameters

In order to compare the computational load of the three parameter computation methods, we measured the average time that each method took to determine the value of the gains and Doppler frequencies of the simulation model by considering $N \in \{10, 20, 30, 40, 50, 100\}$. The results are presented in Table I. It can clearly be seen from Table I that the RSM is by far less time-consuming than the GMEA and the LPNM.

It is important to mention that the complexity of the SOC channel simulator depends only on the number of cisoids N, and it is therefore not influenced by the characteristics of the parameter computation methods. Hence, for a given value of N, the simulator's complexity proves to be the same irrespective of the computational load of the chosen parameter computation method.

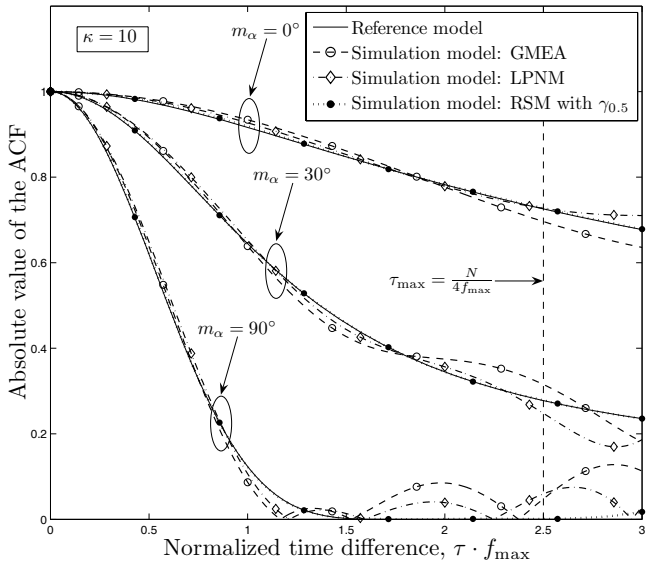

Fig. 2. Comparison among the GMEA, the LPNM, and the RSM in terms of the emulation of the reference model's ACF by considering the von Mises PDF of the AOA with parameters $m_\alpha \in \{0°, 30°, 90°\}$ and $\kappa = 10$ ($N = 10$, $f_{\max} = 91$ Hz, $\sigma^2_{\boldsymbol{\mu}} = 1$, $p = 2$, $\tau_{\max} = N/(4f_{\max})$).

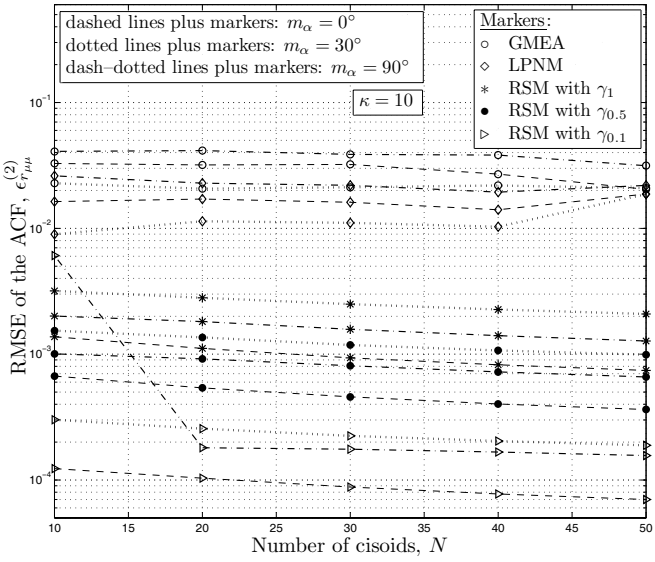

Fig. 3. RMSE $\epsilon^{(2)}_{r_{\boldsymbol{\mu}\boldsymbol{\mu}}}$ of the ACF of the SOC simulation model designed by applying the RSM, the GMEA, and the LPNM on the von Mises PDF with parameters $m_\alpha \in \{0°, 30°, 90°\}$ and $\kappa = 10$ ($f_{\max} = 91$ Hz, $\sigma^2_{\boldsymbol{\mu}} = 1$, $p = 2$, $\tau_{\max} = N/(4f_{\max})$).

VI. Summary and Conclusions

In this paper, we introduced the RSM as an effective parameter computation method enabling the design of SOC simulation models for narrowband mobile Rayleigh fading channels under non-isotropic scattering conditions. The results

TABLE I
AVERAGE TIME REQUIRED FOR COMPUTING THE GAINS AND DOPPLER FREQUENCIES OF THE SOC SIMULATION MODEL ($\sigma_{\boldsymbol{\mu}}^2 = 1$, $f_{\max} = 91$ Hz, AND $\tau_{\max} = N/(4f_{\max})$).

	Average time† (in seconds) by considering:					
Method	$N = 10$	$N = 20$	$N = 30$	$N = 40$	$N = 50$	$N = 100$
GMEA	0.37	0.73	1.09	1.46	1.86	3.72
LPNM	7.48	25.26	51.29	88.23	153.90	545.44
RSM	0.002	0.002	0.002	0.002	0.002	0.003

†The time was measured by employing an off-the-shelf notebook with an Intel® Core™ 2 Duo processor with a 2.5 GHz clock speed.

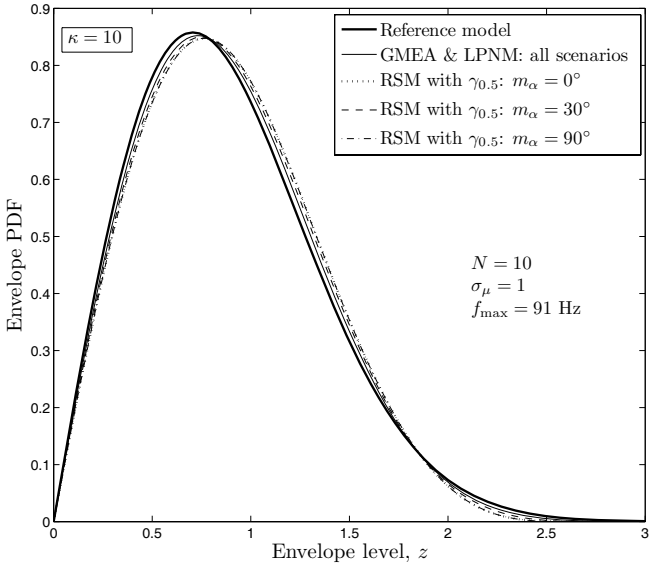

Fig. 4. Comparison between the envelope PDF of the reference model and the envelope PDF of simulation model by applying the GMEA/LPNM and the RSM on the von Mises PDF with $m_\alpha \in \{0°, 30°, 90°\}$ and $\kappa = 10$.

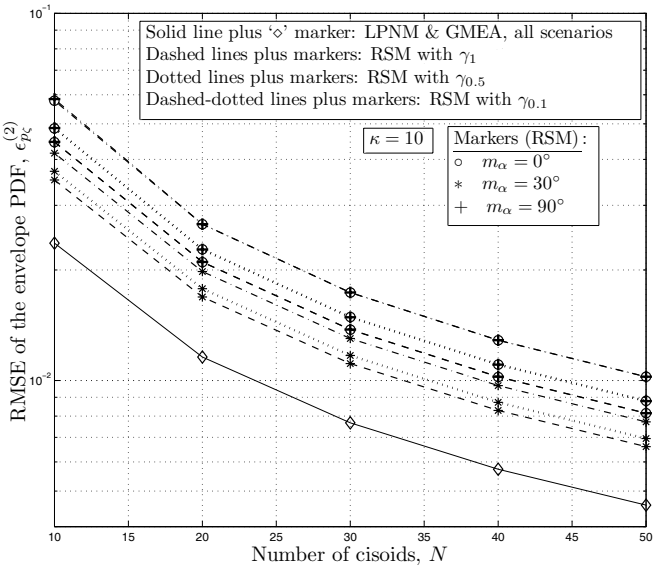

Fig. 5. RMSE $\epsilon_{p\zeta}^{(2)}$ of the envelope PDF of the simulation model designed by applying the RSM, the GMEA, and the LPNM on the von Mises PDF with $m_\alpha \in \{0°, 30°, 90°\}$ and $\kappa = 10$ ($\sigma_{\boldsymbol{\mu}}^2 = 1$, $f_{\max} = 91$ Hz, $p = 2$, $\tau_{\max} = N/(4f_{\max})$).

presented in this paper indicate that the LPNM and the GMEA are more precise than the RSM regarding the approximation of the envelope PDF. However, the RSM is better suited than the other two methods to emulate the channel's correlation characteristics. Furthermore, the overall performance of the RSM can considerably be improved by increasing the number of cisoids N, at the expenses of a negligible increment in the time required to compute the model parameters. In contrast, for the GMEA and the LPNM, the obtained results show that increasing N does not produce a significant improvement on the RMSE of the simulation model's ACF. What is more, in the case of the LPNM, the time required to determine the model parameters increases exponentially with N. In addition to its efficiency and good performance, the simplicity of the RSM makes this method a suitable tool for the design of simulation platforms for the analysis of modern mobile wireless communication systems.

ACKNOWLEDGMENTS

The work by C. A. Gutiérrez was financed in part by the Mexican National Council for Science and Technology (CONACYT). The authors are grateful to the associate editor, Dr. K. K. Wong, and the anonymous reviewers for their helpful comments and constructive criticism.

REFERENCES

[1] A. Abdi, H. Zhang, and C. Tepedelenlioglu, "A unified approach to the performance analysis of speed estimation techniques in mobile communication," *IEEE Trans. Wireless Commun.*, vol. 56, no. 1, pp. 126–135, Jan. 2008.

[2] M. Pätzold and N. Youssef, "Modelling and simulation of direction-selective and frequency-selective mobile radio channels," *Int. J. Electron. Commun.*, vol. AEÜ-55, no. 6, pp. 433–442, Nov. 2001.

[3] C. A. Gutiérrez and M. Pätzold, "Sum-of-sinusoids-based simulation of flat-fading wireless propagation channels under non-isotropic scattering conditions," in *Proc. 50th IEEE Global Commun. Conf. (Globecom 2007)*, Washington, DC, Nov. 2007, pp. 3842–3846.

[4] M. Pätzold, B. O. Hogstad, and N. Youssef, "Modeling, analysis, and simulation of MIMO mobile-to-mobile fading channels," *IEEE Trans. Wireless Commun.*, vol. 7, no. 2, pp. 510–520, Feb. 2008.

[5] H. Zhang, D. Yuan, M. Pätzold, and V. D. Nguyen, "A novel wideband space-time channel simulator based on the geometrical one-ring model with application in MIMO-OFDM systems," *Wireless Commun. Mob. Comput.*, published online March 30, 2009, DOI: 10.1002/wcm.787.

[6] W. R. Braun and U. Dersch, "A physical mobile radio channel model," *IEEE Trans. Veh. Technol.*, vol. 40, no. 2, pp. 472–482, May 1991.

[7] C. A. Gutiérrez, *Channel Simulation Models for Mobile Broadband Communication Systems*. Kristiansand: University of Agder, 2009.
[8] A. Abdi, J. A. Barger, and M. Kaveh, "A parameteric model for the distribution of the angle of arrival and the associated correlation function and power spectrum at the mobile station," *IEEE Trans. Veh. Technol.*, vol. 51, no. 3, pp. 425–434, May 2002.
[9] R. H. Clarke, "A statistical theory of mobile radio reception," *Bell Syst. Tech. J.*, vol. 47, pp. 957–1000, July 1968.
[10] A. Leon-Garcia, *Probability and Random Processes for Electrical Engineering*, 2nd ed. New York: Addison-Wesley, 1994.
[11] M. Pätzold, *Mobile Fading Channels*. Chichester, UK: John Wiley and Sons, 2002.
[12] K. V. Mardia and P. E. Jupp, *Directional Statistics*. Chichester, UK: John Wiley and Sons, 1999.
[13] M. Pätzold and B. Talha, "On the statistical properties of sum-of-cisoids-based mobile radio channel simulators," in *Proc. 10th Int. Symp. on Wireless Personal Multimedia Communications (WPMC'07)*, Jaipur, India, Dec. 2007.
[14] C. A. Gutiérrez and M. Cabrera-Bean, "Deterministic simulation of flat-fading MIMO wireless channels under non-isotropic scattering conditions," in *Proc. 17th IEEE Int. Symp. on Personal, Indoor, and Mobile Radio Commun. (PIMRC'07)*, Athens, Greece, Sep. 2007.
[15] J. K. Patel and C. B. Read, *Handbook of the Normal Distribution*, 2nd ed. New York: CRC Press, 1996.
[16] K. I. Pedersen, P. E. Mogensen, and B. H. Fleury, "Power azimuth spectrum in outdoor environments," *IEE Electron. Lett.*, vol. 33, no. 18, pp. 1583–1584, Aug. 1997.
[17] J. C. Lagarias, J. A. Reeds, M. H. Wright, and P. E. Wright, "Convergence properties of the Nelder–Mead simplex method in low dimensions," *SIAM J. Optimization*, vol. 9, no. 1, pp. 112–147, 1998.